Thermal behavior and structural study of ZrO_2/poly(ε-caprolactone) hybrids synthesized via sol-gel route

Michelina Catauro[1], Elisabetta Tranquillo [1], Alessandro Dell'Era[2], Riccardo Tuffi[3], Stefano Vecchio Ciprioti[2,*]

[1] *Department of Engineering, University of Campania "Luigi Vanvitelli", via Roma 29, Aversa (CE), Italy.*

[2] *Department of Basic and Applied Science for Engineering (S.B.A.I.), Sapienza University of Rome, via del Castro Laurenziano 7, Roma, Italy*

[3] *Department of Sustainability, ENEA – Casaccia Research Center, Via Anguillarese 301, Rome, Italy*

*Corresponding author: Dr. Stefano Vecchio Ciprioti
Department of Basic and Applied Science for Engineering (S.B.A.I.)
Sapienza University of Rome
Via del Castro Laurenziano 7,
Building RM017, I-00161 Rome, Italy.
stefano.vecchio@uniroma1.it
Phone: 0039 0649766906
Fax: 0039 0649766749

Abstract:

The thermal behavior of pure ZrO_2 and four ZrO_2-based organic-inorganic hybrids (OIHs) containing increasing amount (6, 12, 24 and 50 wt%) of poly(ε-caprolactone) (PCL) (named Z, ZP6, ZP12, ZP24 and ZP50 respectively) has been studied by simultaneous thermogravimetry (TG) and differential scanning calorimetry (DSC). The FTIR analysis of the gas mixture evolved at defined temperatures from the samples submitted to the TG experiments identified the mechanism of each thermally activated process. The obtained results suggest that the inorganic matrix of the OIHs prepared by this method exerts a stabilizing effect on the polymer, in particular for poor-PCL hybrid materials. In fact, the different thermal behavior of the ZP50 sample suggests that the polymer is not entirely bonded to the -OH groups of the zirconia matrix due to their saturation. For this reason a part of PCL is not affected by the stabilizing effect of the matrix and is subjected to thermal degradation. Finally, by observing their thermal behavior it was possible to select the most suitable temperatures for thermal pretreatment: 400, 600 and 1000°C. The structural analysis by X-ray diffraction (XRD) revealed that at 400°C the materials are amorphous, while at 600°C they are mostly tetragonal, and the content of the tetragonal phase decreases with increasing the amount of PCL in the OIHs. All the materials treated at 1000°C are monoclinic, but their crystallinity decreases with increasing the PCL content.

Keywords: Sol-gel method; ZrO_2–based hybrids; poly(ε-caprolactone); Coupled TG-FTIR analysis; X-ray Diffraction analysis

Introduction

Organic-inorganic hybrids (OIHs) belong to an important class of materials consisting of organic and inorganic components intimately mixed at a nanometric scale through weak hydrogen bonds or van der Waals forces (Class I), or strong chemical bonds (covalent or ionic covalent bonds, Class II) [1-3]. As a consequence, their properties are not simply the sum of those of the single components, but exert synergetic or complementary effects of the two phases, becoming suitable for several biomedical applications [4-7], with particular reference to bone repair and substitution [8, 9].

Zirconia and zirconia-based glasses and ceramic materials have attracted increasing interest due to their remarkable biological and mechanical properties [10-13], which make them suitable to be used in the biomedical field. In particular, after in vivo implantation of zirconia prostheses and subsequent encapsulation by connective tissues, no local or systemic toxic effects were recorded [7, 10-14], although it is recognized as a bioinert material: it does not show either the ability of direct bone bonding or osteoconduction behavior.

An ideal technique to prepare OIHs is the sol-gel methods, a versatile synthesis process used to produce glasses and ceramics at low temperatures through a transition of the system from a colloidal liquid ('sol') into a solid 'gel', involving hydrolysis of a metal alkoxide precursor and polycondensation reactions occurring in a water-alcohol solution [15, 16]. The low processing temperature allows entrapping thermolabile molecules (e.g. polymers and drugs) in the inorganic matrix, thus producing OIHs. When a hybrid material is developed the main effort is focused on trying to overcome the disadvantages of both the components and to retain their advantages. In particular, the leading idea in the development of a zirconia-based organic-inorganic hybrid is to retain the bioactivity and biocompatibility of the zirconia matrix and to decrease its brittleness by adding a polymer with good mechanical properties.

Recently, our group has been involved in studying bioactive and biocompatible ZrO_2-based OIHs, with particular reference to ZrO_2/hydroxyapatite (ZrO_2/HAp) [17], and

ZrO_2/polycaprolactone (ZrO_2/PCL), hybrids containing increasing percentages of the organic component (6, 12, 24 and 50 wt%) [7, 18-21], starting from their syntheses via the sol-gel process, followed by their characterization by means of several thermoanalytical and spectroscopic techniques. During the last years, the study carried out on the ZrO_2/HAp hybrids [17], as well as those about other similar materials [22], showed that the biological properties of the developed sol-gel systems can be modulated by the modification of the thermal treatment carried out on the obtained gels. The thermal treatment is necessary to remove residual solvents and water from the gels and can lead to a reorganization of the material structure. Amorphous zirconia, for example, can evolve to tetragonal, monoclinic or cubic crystalline forms, which have different properties. The temperature and the heating rate used are key factors able to affect the final structure of the sol-gel materials (porosity, crystallinity degree, etc.) and, thus, their biological properties [8, 17, 23]. Cell adhesion and bioactivity (the ability of inducing HAp nucleation and, thus, osseointegration), indeed, are influenced by surface topography and ion release ability [24-26], which depend on the materials structure.

Therefore, the aim of the present work has been to investigate the thermal behavior of the amorphous bioactive and biocompatible sol-gel ZrO_2/PCL materials in order to choose the most suitable conditions to carry out their thermal treatments to obtain material structural modifications. The knowledge of such information can be useful for developing ZrO_2/PCL materials with different microstructure that, in a future study, could exhibit biological properties different from the amorphous ZrO_2/PCL materials. In order to confirm that structural modifications induced upon heating take place and to identify the new phases formed, X-Ray Diffraction (XRD) analysis was carried out on fresh samples as well as on those treated at three suitable high temperatures.

So, a careful study of the degradation phenomena occurring in the hybrid materials and in which the polymer is involved upon heating was performed using a multi-technique approach, similarly to what has been carried out in the recent past using thermal analysis and X-ray spectroscopies [27] or thermogravimetry coupled with Fourier transform infrared spectroscopy (TG/FTIR) [28] or to Mass

spectrometry (TG/MS) [29] to analyze the gases evolved during the TG experiments and to elucidate the mechanisms of degradation.

Although the thermal degradation of PCL was widely investigated in the past [30-33], indeed, it is not possible to predict the thermal behavior of the hybrids by comparing simply those of the pure organic and inorganic components taken from the literature, because the polymer embedded in the inorganic matrix, the formation of chemical bonds between the organic and the inorganic components of the hybrids and the nature of such bonds can lead to new materials, whose properties, in particular the thermal behavior is a priori unknown.

Material and methods

Pure ZrO_2 (hereinafter denoted as Z) and inorganic/organic ZrO_2/PCL hybrids materials containing 6, 12, 24, and 50 wt% of the organic component (hereinafter denoted as ZP6, ZP12, ZP24 and ZP50 respectively), were synthesized by the sol-gel process. A zirconium(IV) propoxide solution ($Zr(OC_3H_7)_4$ 70 wt% in n-propanol, Sigma Aldrich) and PCL (average molar mass of 10,000 g mol^{-1}, Sigma Aldrich) were used as inorganic and organic precursors respectively. A 1.04 M solution of $Zr(OC_3H_7)_4$ was added to a mixture of ethanol (EtOH, 99.8%, Sigma-Aldrich) and acetylacetone (AcAc, Sigma-Aldrich). AcAc was added to control the hydrolytic activity of zirconium alkoxide. The molar ratios among the reagents achieved in the mixture are: $EtOH/Zr(OC_3H_7)_4$ = 8.1 $Zr(OC_3H_7)_4$/AcAc = 3.1. That mixture, then, was added to chloroform solutions of PCL with concentration 1.46 mM, 1.49 mM, 1.90 mM and 4.00 mM to synthesize ZP6, ZP12, ZP24 and ZP50, respectively.

The solution was kept under magnetic stirring and the resulting sols were uniform and homogeneous. After gelation, all wet gels were air dried at 45°C for 48 h to remove the residual solvents and no traces of any polymer degradation were found.

Subsequently, all the samples were reduced to fine powders by gently grinding them in an agate mortar for some minutes. Then, the obtained powder samples were further characterized by coupled

thermogravimetry/Fourier transform infrared spectroscopy (TG/FTIR), coupled TG/Differential scanning calorimetry (TG/DSC) and X-ray diffraction (XRD) analyses.

The thermal behavior of the OIHs was studied using a simultaneous Mettler Toledo TG/DSC 2950 instrument, equipped with a STARe software. The instrument has been equipped with two identical cylindrical crucibles, one for the reference filled with alumina in powder form and one for the sample, uniformly covered with about 20–25 mg of solid to uniformly cover the bottom surface area of a crucible. The TG/DSC experiments were carried out under an inert nitrogen flowing atmosphere (60 mL min^{-1}) up to 700 °C at a heating rate of 10°C min^{-1}. Calibration of the sample temperature was performed using very pure indium and zinc reference materials (purity higher than 99.998%), thus assuming a final average uncertainty $u(T)=\pm 1$K was estimated over the whole temperature range.

In order to elucidate the mechanism of thermally activated processes occurring in the OIHs during the TG/DSC experiments, the TG/FTIR experiments were carried out using a SETARAM 92-16.18 TG apparatus under a stream of argon of 40 mL min^{-1} in the temperature range between 25 and 700°C at 10°C min^{-1}. This instrument has been equipped with 250 μL alumina crucibles filled with about 100-150 mg of sample to obtain the minimum amount of gaseous species to be analyzed by FTIR measurements. A preliminary blank experiment was performed using empty crucibles under the same experimental conditions of the samples tested. All the experimental data were collected and analyzed using the Calisto software. The vapors evolved during the TG experiments were conveyed to a Thermofisher Scientific Nicolet iS10 Spectrophotometer linked through a heated transfer line kept at 200°C. The instrument allows monitoring the actual reaction trend by collecting a spectrum each 11 s, being eight scans performed at 0.5 cm^{-1} intervals with a resolution of 4 cm^{-1}.

The morphology of the synthesized gel materials was investigated by scanning electron microscopy analysis performed using an AURIGA Zeiss High Resolution Field Emission (HR-FESEM).

After a thermal treatment of the samples powders at 400, 600 and 1000°C (temperatures selected on the basis of a careful examination of their thermal behavior shown by the TG experiments) for 2 h under argon purge gas atmosphere, the crystalline phases have been identified by XRD analysis using a Philips diffractometer equipped with a PW 1830 generator, tungsten lamp and Cu anode, where the source of X-ray is given by a Cu-Kα radiation (λ=0.15418 nm).

Results and Discussion

Thermal behavior study through TG/DSC and TG/FTIR experiments

The TG/DSC curves of pure ZrO_2 and of the ZrO_2/PCL hybrids have been reported in Fig. 1. Initial and final temperatures of all the processes accompanied by a mass loss are more clearly identified in the first-order derivative curves of TG (DTG) curves displayed in Fig. 2, where a vertical bar close to each DTG peak represents the temperature at which the gas or gases evolved from TG experiments were collected and sent to the FTIR device for the evolution gas analysis (EGA). The FTIR spectra of the gaseous species so collected from TG/DSC experiments of all materials tested at all the temperatures close to the DTG peak temperatures where the reaction reaches the maximum rates (corresponding to a vertical bars in the DTG curves) are shown in Fig. 3. Fig. 1 shows that all the materials undergo a first mass loss (corresponding to the first DTG peak and an endothermic DSC peak) ascribed to loss of alcohol up to 140°C, except for ZP50 (short dotted lines) for which the process is shifted toward lower temperature (ends at around 80°C). The ZP hybrid materials, except the PCL-richest OHI, ZP50, show the same thermal behavior of pure Z.

As far as pure zirconia is concerned, the FTIR spectrum of the gaseous products collected during the TG experiment of pure ZrO_2 at 64°C, close to the corresponding DTG peak showed the release of propanol. This is proved by the presence of the intense bands at 2970 cm^{-1} and 1060 cm^{-1}, with a shoulder at 978 cm^{-1} ascribable to C–H and C–C stretching in the propanol, by the weak signals at 3670 cm^{-1}, due to –OH stretching, and the signals in the region between 1200 and 1500 cm^{-1},

ascribable to the C–H bending modes. This alcohol is produced by hydrolysis and condensation reactions, which involve zirconium propoxide precursor.

Other two steps of mass loss are visible in the TG curve of pure ZrO_2, which is accompanied by several effects in the corresponding DSC curve related to decomposition/oxidation of acetylacetone and crystallization of zirconia [34, 35]. The FTIR spectrum of the gaseous products collected during the TG experiment on pure zirconia at 198°C shows propanol residues as well as the bands corresponding to the wavenumbers equal to 1735 cm^{-1}, 1365 cm^{-1} and 1210 cm^{-1}, are due to C=O, C–H and C–C deformations respectively, prove that acetone also evolved due to the thermal degradation of the acetylacetone bonded to zirconium (acetylacetonate of zirconium) [36]. The bands of propanol and acetone with lower intensity are visible also in the spectrum recorded at 343°C together with the signals typical of the CO_2 (the doublet at 2360 - 2319 cm^{-1} and the sharp peak at 670 cm^{-1}) which, in turn, develops by the degradation of the acetone.

As far as the poor-PCL OHIs (with 6, 12 and 24% of PCL) are concerned, although the polymer is intimately linked to the zirconia matrix, no evidences of thermal degradation of PCL are visible. In previous studies the thermal degradation of PCL was observed to occur in the temperature range between 230 and 470 °C as a function of the polymer chain length [31, 33] and the setting of the instrument used to carry out the thermal analysis (gas carrier, resolution parameters, heating rate [30-33]).

Other two steps of weight loss in the TG curve are visible, coupled with several effects in DSC curve, which are related to the decomposition/oxidation of acetylacetone and the crystallization of zirconia. Also in these samples, for temperature above 300°C, a decrease of the peaks related to propanol and acetone and the development of CO_2, due to the acetone degradation was recorded as observed for Z.

Therefore, although the presence of polymer, no evidences of its thermal degradation are visible. The obtained results suggest that the inorganic matrix exerts a stabilizing effect on the polymer. Moreover, the FTIR spectrum of the gaseous mixture evolved during the TG experiment on ZP12 at

501°C revealed the presence of methane and CO_2, which are obtained by the thermal degradation of acetone [36].

A completely different thermal behavior is observed when 50 wt% of PCL is embedded in the zirconia matrix. In particular, no trace of propanol is found in the FTIR spectrum collected from the gas released during the TG experiment of ZP50 at 43°C, whereas that at about 169°C reveals the characteristic bands of acetone along with those of acetylacetone and propanol (in lower amount) at about 1610 cm^{-1} and 1060 cm^{-1}. The formation of ε-caprolactone (the cyclic monomer used to synthesize the PCL) is evident in the FTIR spectrum of the gas collected at 263°C and causes the appearance of the intense endothermic peak recorded in the DSC curve between 200 and 320°C. Its formation is the result of the thermal degradation of PCL and, in particular, of an unzipping depolymerization process, which takes place from the ends of the polymer chains, according with Persenaire at al. [31] and Aoyagi et al. [30]. However, those two research groups proposed two different mechanisms for the thermal degradation of PCL. Persenaire at al. [31] observed two degradation peaks in the DTA curve at temperatures between 230°C and 420°C depending on gas (He and O_2) and polymer chain length. Based on the analysis of the gas evolved, they proposed a two-step mechanism, where the random rupture of the polyester chains via cis-elimination reaction, which leads to the production of H_2O, CO_2, and 5-hexenoic acid, is followed by the unzipping depolymerization process leading to the formation of the ε-caprolactone. Results obtained by Aoyagi et al. [30] in N_2 environment and isothermal conditions show that the degradation takes place at 280°C with one-step mechanism, which is the unzipping depolymerization from the polymer-chain ends. However, Aoyagi et al. do not exclude that also the random rupture of the polyester chains via a cis-elimination reaction occurs, but this process may by undetectable using a traditional low resolution thermal analysis equipment because occurs at a temperature very close that one of the depolymerization.

Therefore, although the mechanism and temperature range of the thermal degradation of PCL is well-known [30-33], a comparison of the results obtained in the present study with those taken from

226 literature is not simple, since the thermal behavior of the hybrids is usually quite different from
227 those of the pure organic and inorganic components. In fact, as stated above, the organic component
228 (i.e., the polymer) embedded in the inorganic matrix via the formation of chemical bonds are new
229 materials, whose properties and thermal behavior are a priori unpredictable. In particular, the
230 reported temperatures that caused the formation of the first degradation products are very different.
231 Unger et al. [32] in nitrogen atmosphere and using heating rate of 10°C/min (conditions similar to
232 those used in the present study) reported that the thermal degradation of PCL (average molecular
233 weight of 10000) starts at 280°C leading to the formation of ε-caprolactone and 5-hexenoic acid at
234 higher temperature. The recorded different thermal behavior of ZP50 and the formation of the first
235 degradation products at 263°C, in the present work, thus, suggest that when a significant amount of
236 PCL is present in the OIH materials, the polymer is not completely bonded to the –OH groups of
237 the zirconia matrix, due to their saturation. For this reason, a part of the PCL is not affected by the
238 stabilizing effect of the matrix and is subjected to thermal degradation following a behavior very
239 similar to that of pure PCL. Therefore, the obtained results confirm that when the polymer is linked
240 to the inorganic matrix, the formed hybrid is a new material with its own thermal behavior and
241 within the hybrid the organic component do not retain its thermal behavior. On the contrary, the
242 PCL moieties not linked through chemical bonds to the inorganic matrix behave similarly to pure
243 PCL. Moreover, the significant weight loss recorded for ZP50 below 300°C is ascribable to the
244 degradation of the synthesis residues retained in the inorganic matrix (acetyl acetone and solvents,
245 as well as recorded in the other samples) and to the free PCL (not linked to the zirconia matrix).
246 Moreover, the formation of 5-hexenoic acid, undetected under the used experimental condition,
247 cannot be excluded.

248 The saturation of the –OH groups explains also the lower content of propanol, not thermally
249 released at lower temperature. The dehydroxylation process that generally takes place in these
250 materials upon heating, leading to the formation of new O-bridging bonds with the production of
251 propanol or water, indeed, is hindered due to the absence of free –OH groups.

252 The spectra recorded at higher temperature (380 and 475°C) show a decrease in the intensity of
253 the ε-caprolactone band and an increase of that of CO_2. This result can be explained by the
254 occurrence of degradation of the ε-caprolactone, which leads to the formation of CO_2.
255
256 **Structural study of the solid phases after the thermal treatments of the OIHs**
257 The morphology of untreated and thermally treated OIHs (Figs. 4 and 5) was observed by carrying
258 out HR-FESEM measurements. Fig. 4 shows the micrographs of the untreated samples recorded at
259 high magnification. All the fresh materials have a compact morphology and proved that the organic
260 and inorganic components are interpenetrated on nanometric scale. Therefore, all the samples are
261 homogeneous and no phase separation is visible under 1μm, confirming that the synthesized
262 materials are hybrids, according to the IUPAC definition [37]. SEM images of the samples acquired
263 after heat treatments (Fig. 5), show that heating up to 600°C does not cause significant
264 morphological modifications, whereas the thermal treatment at 1000°C leads to a new morphology,
265 with a structure similar to particle agglomerates.
266 The XRD spectra shown in Figs. 6-9 reveal that the structure of all the OIH samples depends on the
267 temperature of the thermal treatment. In particular, the samples treated at 400°C (Fig. 6) are
268 amorphous, and the content of the amorphous phase in the OIHs treated at 400°C slightly decreases
269 with increasing the amount of PCL. This can be due to the crystalline nature of the pure PCL [38].
270 By observing carefully Fig. 7, it is worth noting to stress that the hybrid materials treated at 600°C
271 have a prevailing tetragonal crystalline structure, and the appearance of the monoclinic phase
272 depends on the amount of PCL in the OIH: the higher is the amount of PCL, the higher is the
273 content of the monoclinic phase in the material [39-42]. The Crystallographic Open Database
274 (C.O.D.), an open-access collection of crystal structures of organic, inorganic, metal-organics
275 compounds and minerals, excluding biopolymers) was used to identify the monoclinic and
276 tetragonal phases of zirconia (denoted as *m*-ZrO_2 and *t*-ZrO_2, respectively) were identified (with
277 C.O.D. codes equal to 9006695 and 9016714, respectively). Since PCL is not considered in this

database it was identified by comparing the peaks of the XRD spectra with those found in literature [43, 44]. The same procedure was carried out for all the materials, and the XRD spectrum of ZP50 has been reported in Fig. 8 as an example.

The percentage of the monoclinic phase with respect to the tetragonal one has been evaluated for the samples ZP12, ZP24 and ZP50 treated at 600°C according to Eq. (1) proposed in previous studies [40, 42]:

$$x=[I_m(11\text{-}1)+I_m(111)]/[I_m(11\text{-}1)+I_m(111)+I_t(101)] \quad (1)$$

where $I_m(11\text{-}1)$ and $I_m(111)$ represent the areas under the peaks (integrated intensity) related to (11-1) and (111) of the monoclinic phase, while $I_t(101)$ is that of the tetragonal one, respectively. The percentages of the monoclinic phase in the samples ZP12, ZP24 and ZP50 so determined have been found to be 11.1, 20.8 and 23.2%, respectively. The increase of the content of the monoclinic phase with increasing the amount of PCL can be attributed to the strongest interactions between the PCL carbonyl and OH- groups, obtained according to Sato and Shimada [45] on reaction between water and Zr-O-Zr bonds on the surface, resulting in the formation of OH-groups which in turn cause the release of the strain, acting in stabilizing the metastable *t*-ZrO_2 phase [46]. This interaction could make less effective the stabilizing effect of the OH- groups, thus favoring the m-phase, thermodynamically more stable.

Finally, all the samples heated up to 1000°C show a monoclinic structure (Fig. 9), but the intensity of the peaks decreases with increasing the amount of PCL from pure ZrO_2 to ZP50. It is worth noting that the crystallite size of the samples treated at 600 and 1000°C does not depend on the amount of PEG in the material (Fig. 10): practically constant values have been found within the estimated uncertainties, equal to 43 and 10 nm, respectively.

Conclusions

303 The sol-gel method is a versatile process that allows synthesizing different organic-inorganic
304 hybrid materials, such as organic/inorganic ZrO_2/PCL hybrids containing 6, 12, 24, and 50 wt% of
305 the organic component. The obtained results suggest that the inorganic matrix of the OIHs prepared
306 by this method exerts a stabilizing effect on the polymer, in particular with poor-PCL hybrid
307 materials. In fact, the different thermal behavior of the ZP50 sample suggests that the polymer is
308 not entirely bonded to the -OH groups of the zirconia matrix due to their saturation. For this reason,
309 a part of PCL is not affected by the stabilizing effect of the matrix and is subjected to thermal
310 degradation. Morphological observation carried out by SEM proved that no phase separation is
311 visible in the samples also when 50wt% of polymer is incorporated. Moreover, this analysis showed
312 that the materials are homogeneous before and after the thermal treatment at 400, 600 and 1000 °C,
313 confirming that they are organic-inorganic hybrid materials. However, the samples appear compact
314 up to 600°C heating but after 1000°C heating are subjected to a morphological modification which
315 leads to a particle agglomerates-like structure. That modification is ascribable to the crystalline
316 phase transition which take place in the zirconia matrix after 1000°C heating, since it is observed
317 also in the PCL-free samples (Z). The structural analysis by X-ray diffraction (XRD) revealed that
318 the material structures changed from amorphous (at 400°C) to mostly tetragonal mixed to
319 monoclinic (at 600°C). Moreover, the content of the metastable tetragonal phase decreases with
320 increasing the amount of PCL in the OIHs due to strongest interactions occurring between the PCL
321 carbonyl and OH- groups when water reacts with the surface Zr-O-Zr bonds. This result makes less
322 effective the stabilizing effect of the OH- groups, thus favoring the thermodynamically more stable
323 *m*-ZrO_2. After heating all the materials at 1000°C a complete conversion from tetragonal to
324 monoclinic phase took place, while the crystallite size of the samples treated at higher temperatures
325 (600 and 1000°C) seems not to depend on the amount of PCL in the hybrid material.
326 Finally, the obtained results correlated with further investigation about the biological properties
327 of the ZrO_2/PCL hybrids as a function of the heating temperature can be important information for
328 the design of innovative OIH biomaterials.

329

330 **Conflicts of Interest**: All the authors that they have no competing interests.

References:

[1] P. Judeinstein, C. Sanchez, Hybrid organic-inorganic materials: a land of multidisciplinarity, Journal of Materials Chemistry, 6 (1996) 511-525.

[2] C. Sanchez, F. Ribot, Design of hybrid organic-inorganic materials synthesized via sol-gel chemistry, New J. Chem., 18 (1994) 1007-1047.

[3] Y. Wei, D. Jin, D.J. Brennan, D.N. Rivera, Q. Zhuang, N.J. DiNardo, K. Qiu, Atomic Force Microscopy Study of Organicâ'Inorganic Hybrid Materials, Chemistry of Materials, 10 (1998) 769-772.

[4] Q. Chen, N. Miyata, T. Kokubo, T. Nakamura, Bioactivity and mechanical properties of PDMS-modified $CaO-SiO_2-TiO_2$ hybrids prepared by sol-gel process, J. Biomed. Mater. Res., 51 (2000) 605-611.

[5] N. Miyata, K.-i. Fuke, Q. Chen, M. Kawashita, T. Kokubo, T. Nakamura, Apatite-forming ability and mechanical properties of PTMO-modified $CaO-SiO_2$ hybrids prepared by sol-gel processing: effect of CaO and PTMO contents, Biomaterials, 23 (2002) 3033-3040.

[6] M. Catauro, F. Bollino, F. Papale, C. Ferrara, P. Mustarelli, Silica-polyethylene glycol hybrids synthesized by sol-gel: Biocompatibility improvement of titanium implants by coating, Materials Science and Engineering C, 55 (2015) 118-125.

[7] M. Catauro, S. Pacifico, Synthesis of bioactive chlorogenic acid-silica hybrid materials via the sol-gel route and evaluation of their biocompatibility, Materials, 10 (2017).

[8] M. Catauro, R.A. Renella, F. Papale, S. Vecchio Ciprioti, Investigation of bioactivity, biocompatibility and thermal behavior of sol-gel silica glass containing a high PEG percentage, Materials Science and Engineering C, 61 (2016) 51-55.

[9] M. Vallet-Regí, D. Arcos, Nanostructured hybrid materials for bone tissue regeneration, Current Nanoscience, 2 (2006) 179-189.

[10] C. Piconi, G. Maccauro, Zirconia as a ceramic biomaterial, Biomaterials, 20 (1999) 1-25.

[11] O.S. Abd El-Ghany, A.H. Sherief, Zirconia based ceramics, some clinical and biological aspects: Review, Future Dental Journal, 2 (2016) 55-64.

[12] H. Harianawala, M. Kheur, S. Kheur, T. Sethi, A. Bal, M. Burhanpurwala, F. Sayed, Biocompatibility of Zirconia, Journal of Advanced Medical and Dental Sciences Research, 4 (2016) 35-39.

[13] T.R. Ramesh, M. Gangaiah, P.V. Harish, U. Krishnakumar, B. Nandakishore, Zirconia Ceramics as a Dental Biomaterial – An Over view, Trends in Biomaterials and Artificial Organs, 26 (2012) 154-160.

[14] M. Catauro, F. Bollino, F. Papale, Biocompatibility improvement of titanium implants by coating with hybrid materials synthesized by sol-gel technique, Journal of Biomedical Materials Research - Part A, 102 (2014) 4473-4479.

[15] C. Brinker, G. Scherer, Sol-Gel Science: the Physics and Chemistry of Sol-Gel processing, Academic press, San Diego 1989.

[16] M. Catauro, G. Laudisio, A. Costantini, R. Fresa, F. Branda, Low Temperature Synthesis, Structure and Bioactivity of $2CaO{\cdot}3SiO_2$ Glass, Journal of Sol-Gel Science and Technology, 10 (1997) 231-237.

[17] F. Bollino, E. Armenia, E. Tranquillo, Zirconia/hydroxyapatite composites synthesized via sol-gel: Influence of hydroxyapatite content and heating on their biological properties, Materials, 10 (2017).

[18] M. Catauro, F. Bollino, F. Papale, Response of SAOS-2 cells to simulated microgravity and effect of biocompatible sol-gel hybrid coatings, Acta Astronautica, 122 (2016) 237-242.

[19] M. Catauro, F. Bollino, F. Papale, P. Mozetic, A. Rainer, M. Trombetta, Biological response of human mesenchymal stromal cells to titanium grade 4 implants coated with PCL/ZrO_2 hybrid materials synthesized by sol-gel route: In vitro evaluation, Materials Science and Engineering C, 45 (2014) 395-401.

[20] M. Catauro, F. Bollino, P. Veronesi, G. Lamanna, Influence of PCL on mechanical properties and bioactivity of ZrO_2-based hybrid coatings synthesized by sol-gel dip coating technique, Materials Science and Engineering C, 39 (2014) 344-351.
[21] M. Catauro, E. Tranquillo, M. Illiano, L. Sapio, A. Spina, S. Naviglio, The influence of the polymer amount on the biological properties of PCL/ZrO_2 hybrid materials synthesized via sol-gel technique, Materials, 10 (2017).
[22] M. Catauro, F. Bollino, R.A. Renella, F. Papale, Sol-gel synthesis of SiO_2-CaO-P_2O_5 glasses: Influence of the heat treatment on their bioactivity and biocompatibility, Ceramics International, 41 (2015) 12578-12588.
[23] M. Catauro, A. Dell'Era, S. Vecchio Ciprioti, Synthesis, structural, spectroscopic and thermoanalytical study of sol-gel derived SiO_2-CaO-P_2O_5 gel and ceramic materials, Thermochimica Acta, 625 (2016) 20-27.
[24] R. Kumar, H. Münstedt, Polyamide/silver antimicrobials: effect of crystallinity on the silver ion release, Polymer International, 54 (2005) 1180-1186.
[25] E. Mavropoulos, A.M. Costa, L.T. Costa, C.A. Achete, A. Mello, J.M. Granjeiro, A.M. Rossi, Adsorption and bioactivity studies of albumin onto hydroxyapatite surface, Colloids and Surfaces B: Biointerfaces, 83 (2011) 1-9.
[26] L. Radev, Influence of thermal treatment on the structure and in vitro bioactivity of sol-gel prepared CaO-SiO_2-P_2O_5 glass-ceramics, Processing and Application of Ceramics, 8 (2014) 155-166.
[27] S. Vecchio Ciprioti, M. Catauro, Synthesis, structural and thermal behavior study of four Ca-containing silicate gel-glasses, Journal of Thermal Analysis and Calorimetry, 123 (2016) 2091-2101.
[28] S. Materazzi, S. Vecchio Ciprioti, L.W. Wo, S. De Angelis Curtis, TG–MS and TG–FTIR studies of imidazole-substituted coordination compounds: Co(II) and Ni(II)-complexes of bis(1-methylimidazol-2-yl)ketone, Thermochimica Acta, 543 (2012) 183-187.
[29] C. Papadopoulos, N. Kantiranis, S. Vecchio Ciprioti, M. Lalia-Kantouri, Lanthanide complexes of 3-methoxy-salicylaldehyde, Journal of Thermal Analysis and Calorimetry, 99 (2010) 931-938.
[30] Y. Aoyagi, K. Yamashita, Y. Doi, Thermal degradation of poly[(R)-3-hydroxybutyrate], poly[ε-caprolactone], and poly[(S)-lactide], Polymer Degradation and Stability, 76 (2002) 53-59.
[31] O. Persenaire, M. Alexandre, P. Degée, P. Dubois, Mechanisms and Kinetics of Thermal Degradation of Poly(ε-caprolactone), Biomacromolecules, 2 (2001) 288-294.
[32] M. Unger, C. Vogel, H.W. Siesler, Molecular Weight Dependence of the Thermal Degradation of Poly(ε-caprolactone): A Thermogravimetric Differential Thermal Fourier Transform Infrared Spectroscopy Study, Applied Spectroscopy, 64 (2010) 805-809.
[33] C. Vogel, H.W. Siesler, Thermal Degradation of Poly(ε-caprolactone), Poly(L-lactic acid) and their Blends with Poly(3-hydroxy-butyrate) Studied by TGA/FT-IR Spectroscopy, Macromolecular Symposia, 265 (2008) 183-194.
[34] I. Georgieva, N. Danchova, S. Gutzov, N. Trendafilova, DFT modeling, UV-Vis and IR spectroscopic study of acetylacetone-modified zirconia sol-gel materials, J. Mol. Model., 18 (2012) 2409-2422.
[35] S. Vecchio Ciprioti, F. Bollino, E. Tranquillo, M. Catauro, Synthesis, thermal behavior and physicochemical characterization of ZrO_2/PEG inorganic/organic hybrid materials via sol–gel technique, Journal of Thermal Analysis and Calorimetry, 130 (2017) 535-540.
[36] J. Von Hoene, R.G. Charles, W.M. Hickam, Thermal Decomposition of Metal Acetylacetonates: Mass Spectrometer Studies, The Journal of Physical Chemistry, 62 (1958) 1098-1101.
[37] A.D. McNaught, A. Wilkinson, Compendium of Chemical Terminology. Gold Book, 2nd Edition, Blackwell1997.

[38] M. Catauro, F. Bollino, Release kinetics of anti-Inflammatory drug, and characterization and bioactivity of SiO_2+PCL hybrid material synthesized by sol-Gel processing, Journal of Applied Biomaterials and Fundamental Materials, 12 (2014) 218-227.
[39] S.N. Basahel, T.T. Ali, M. Mokhtar, K. Narasimharao, Influence of crystal structure of nanosized ZrO_2 on photocatalytic degradation of methyl orange, Nanoscale research letters, 10 (2015) 73.
[40] A. Behbahani, S. Rowshanzamir, A. Esmaeilifar, Hydrothermal synthesis of zirconia nanoparticles from commercial zirconia, Procedia Engineering, 42 (2012) 908-917.
[41] M. Gauna, M. Conconi, S. Gomez, G. Suarez, E. Aglietti, N. Rendtorff, Monoclinic-tetragonal zirconia quantification of commercial nanopowder mixtures by XRD and DTA, Ceramics–Silikáty, 59 (2015) 318-325.
[42] M. Tahmasebpour, A.A. Babaluo, M.K.R. Aghjeh, Synthesis of zirconia nanopowders from various zirconium salts via polyacrylamide gel method, Journal of the European Ceramic Society, 28 (2008) 773-778.
[43] H.-W. Kim, J.C. Knowles, H.-E. Kim, Hydroxyapatite/poly (ε-caprolactone) composite coatings on hydroxyapatite porous bone scaffold for drug delivery, Biomaterials, 25 (2004) 1279-1287.
[44] M. Shoja, K. Shameli, M. Ahmad, Z. Zakaria, Preparation and characterization of poly (ε-caprolactone)/TiO_2 micro-composites, Digest Journal of Nanomaterials and Biostructures, 10 (2015) 471-477.
[45] T. Sato, M. Shimada, Control of the tetragonal-to-monoclinic phase transformation of yttria partially stabilized zirconia in hot water, Journal of materials science, 20 (1985) 3988-3992.
[46] M. Skovgaard, K. Almdal, A. Van Lelieveld, Stabilization of metastable tetragonal zirconia nanocrystallites by surface modification, Journal of materials science, 46 (2011) 1824-1829.

Captions of the figures

Fig. 1. Simultaneous TG (a) and DSC (b) curves of pure ZrO_2 and of the ZrO_2/PCL hybrids

Fig. 2. DTG curves of pure ZrO_2 and of the ZrO_2/PCL hybrids

Fig. 3. FTIR spectra of the gaseous species evolved during the TG/FTIR experiments of pure ZrO_2 and of the ZrO_2/PCL hybrids.

Fig. 4. HR-FESEM micrographs of untreated: A) Z, B) ZP6, C) ZP12, D) ZP24, E) ZP50.

Fig. 5. HR-FESEM micrographs of representative samples (Z, ZP12 and ZP50) after their treatment at 400°C, 600° and 1000°C.

Fig. 6. XRD spectra of pure ZrO_2 and of the ZrO_2/PCL hybrids treated at 400°C for 2h under a flowing Ar atmosphere.

Fig. 7. XRD spectra of pure ZrO_2 and of the ZrO_2/PCL hybrids treated at 600°C for 2h under a flowing Ar atmosphere.

Fig. 8. Identification of (11-1), (111) and (101) peaks related to monoclinic and tetragonal phases in the XRD spectrum of ZP50 treated at 600°C.

Fig. 9. XRD spectra of pure ZrO_2 and of the ZrO_2/PCL hybrids treated at 1000°C for 2h under a flowing Ar atmosphere.

Fig. 10. Crystallite size of all the materials as a function of the amount of PCL.

Figure 1)

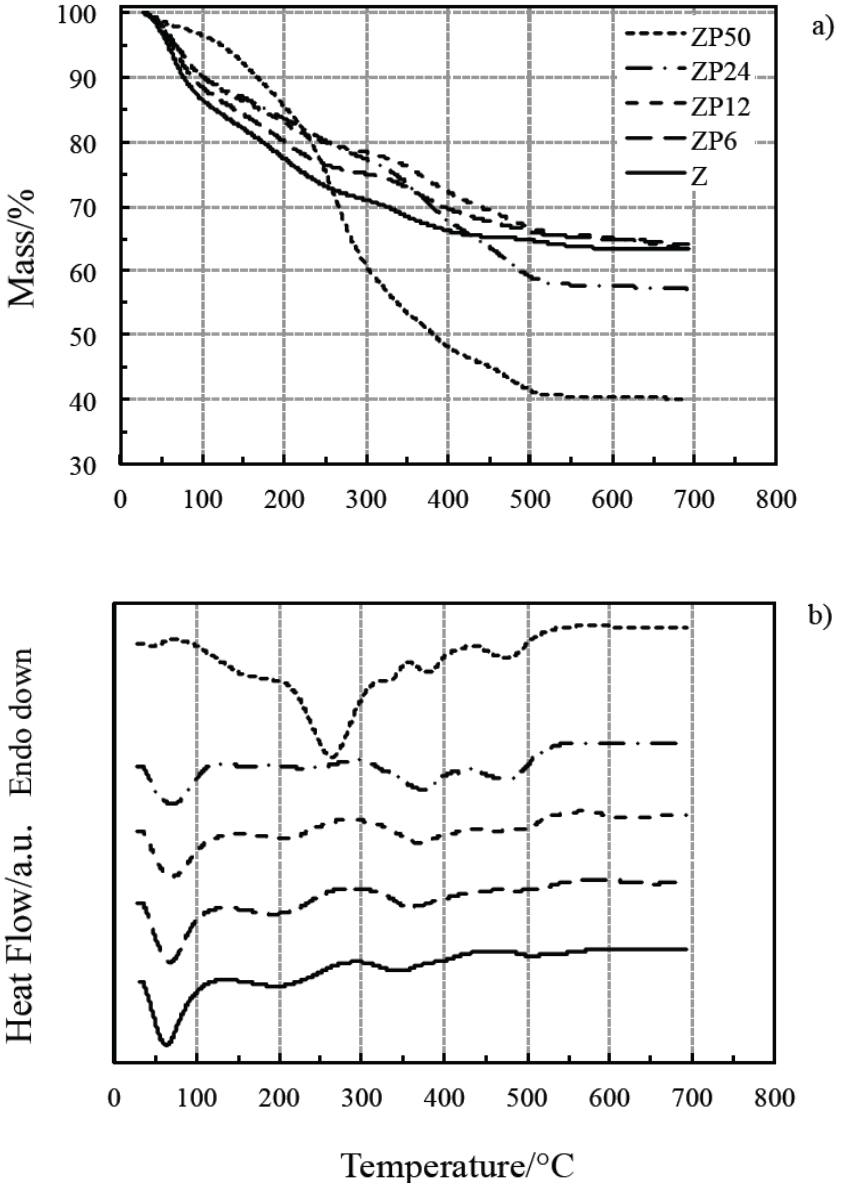
a)
ZP50
ZP24
ZP12
ZP6
Z
Mass/%
100
90
80
70
60
50
40
30
0
100
200
300
400
500
600
700
800
b)
Heat Flow/a.u. Endo down
Temperature/°C

Figure 2)

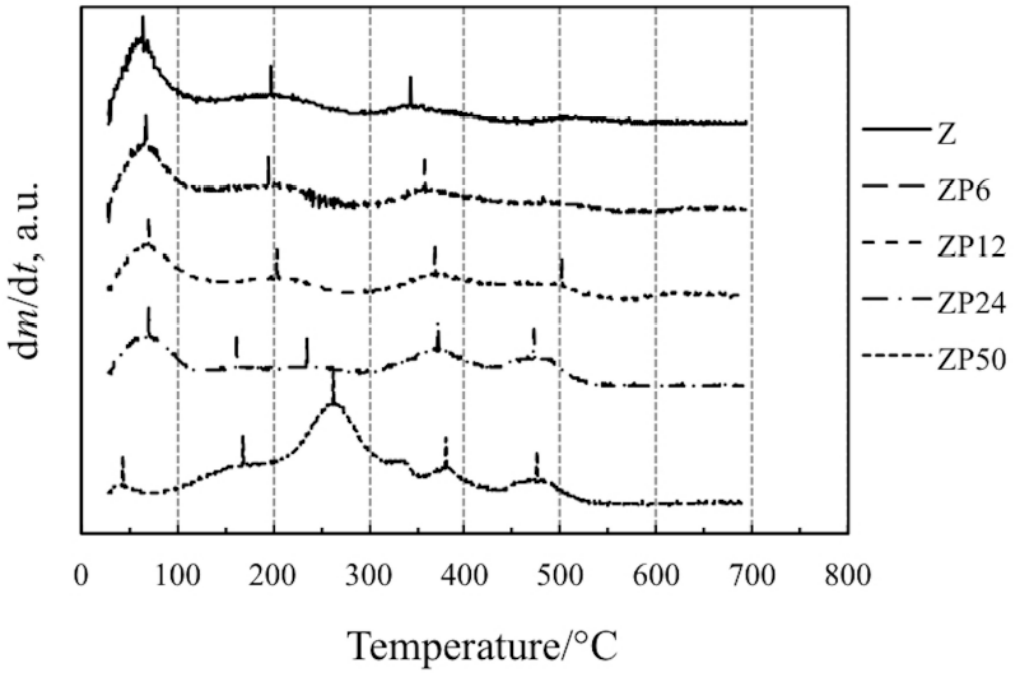
dm/dt, a.u.
0
100
200
300
400
500
600
700
800
Temperature/°C
Z
ZP6
ZP12
ZP24
ZP50

Figure 3)

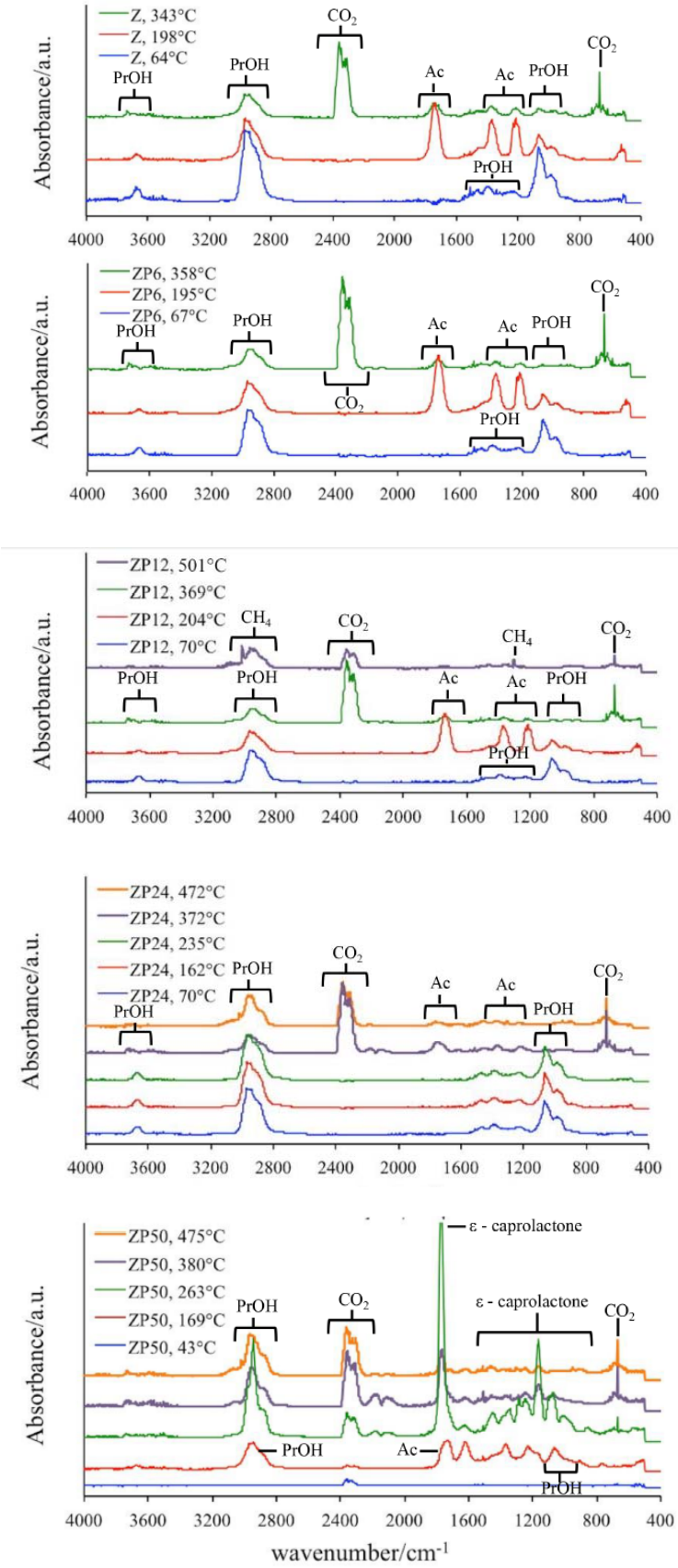
Z, 343°C
Z, 198°C
Z, 64°C
ZP6, 358°C
ZP6, 195°C
ZP6, 67°C
ZP12, 501°C
ZP12, 369°C
ZP12, 204°C
ZP12, 70°C
ZP24, 472°C
ZP24, 372°C
ZP24, 235°C
ZP24, 162°C
ZP24, 70°C
ZP50, 475°C
ZP50, 380°C
ZP50, 263°C
ZP50, 169°C
ZP50, 43°C
PrOH
CO2
Ac
CH4
ε - caprolactone
Absorbance/a.u.
wavenumber/cm-1
4000
3600
3200
2800
2400
2000
1600
1200
800
400

Figure 4)

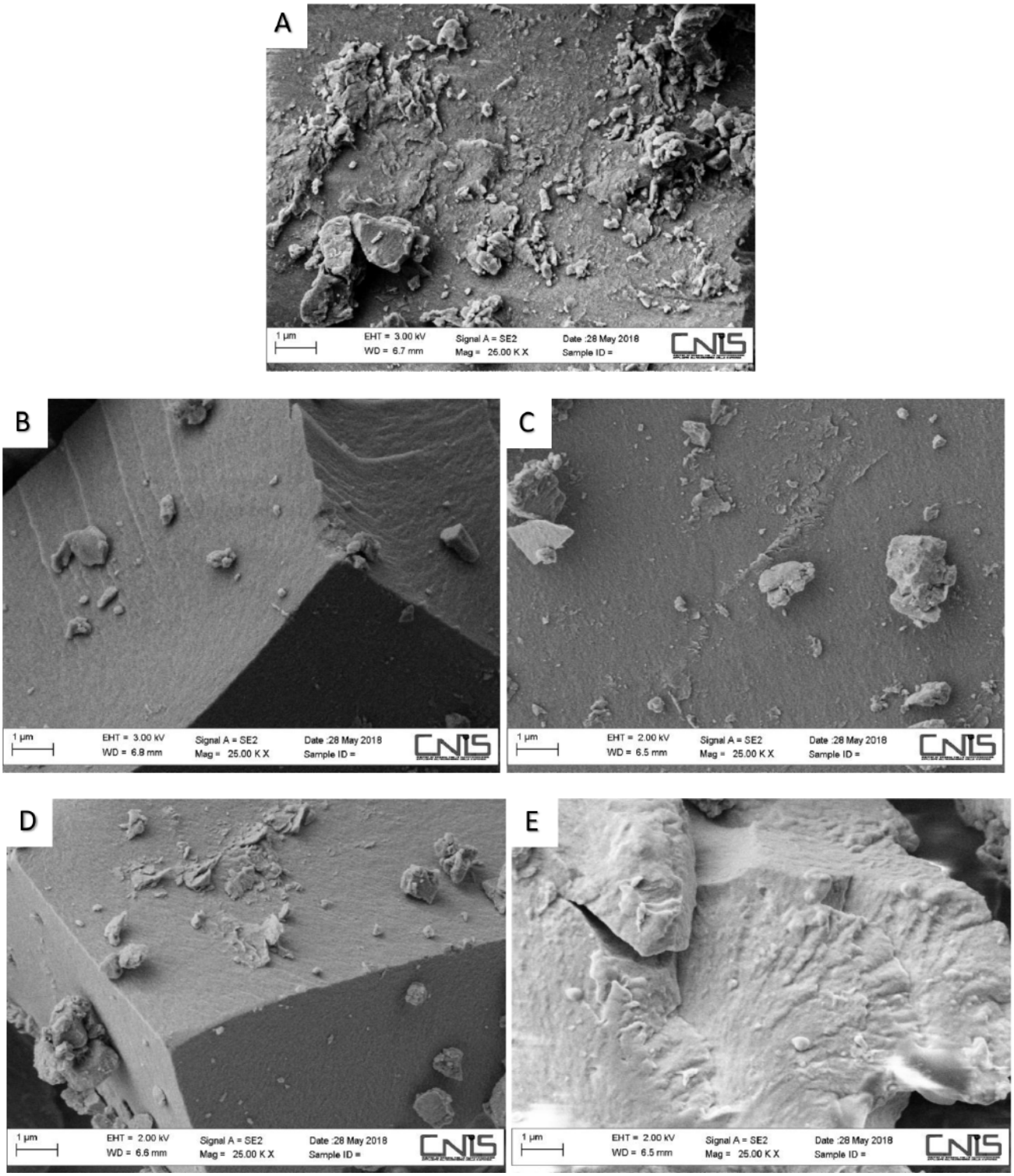
A
1 µm
EHT = 3.00 kV
WD = 6.7 mm
Signal A = SE2
Mag = 25.00 K X
Date :28 May 2018
Sample ID =
B
1 µm
EHT = 3.00 kV
WD = 6.9 mm
Signal A = SE2
Mag = 25.00 K X
Date :28 May 2018
Sample ID =
C
1 µm
EHT = 2.00 kV
WD = 6.5 mm
Signal A = SE2
Mag = 25.00 K X
Date :28 May 2018
Sample ID =
D
1 µm
EHT = 2.00 kV
WD = 6.6 mm
Signal A = SE2
Mag = 25.00 K X
Date :28 May 2018
Sample ID =
E
1 µm
EHT = 2.00 kV
WD = 6.5 mm
Signal A = SE2
Mag = 25.00 K X
Date :28 May 2018
Sample ID =

Figure 5)

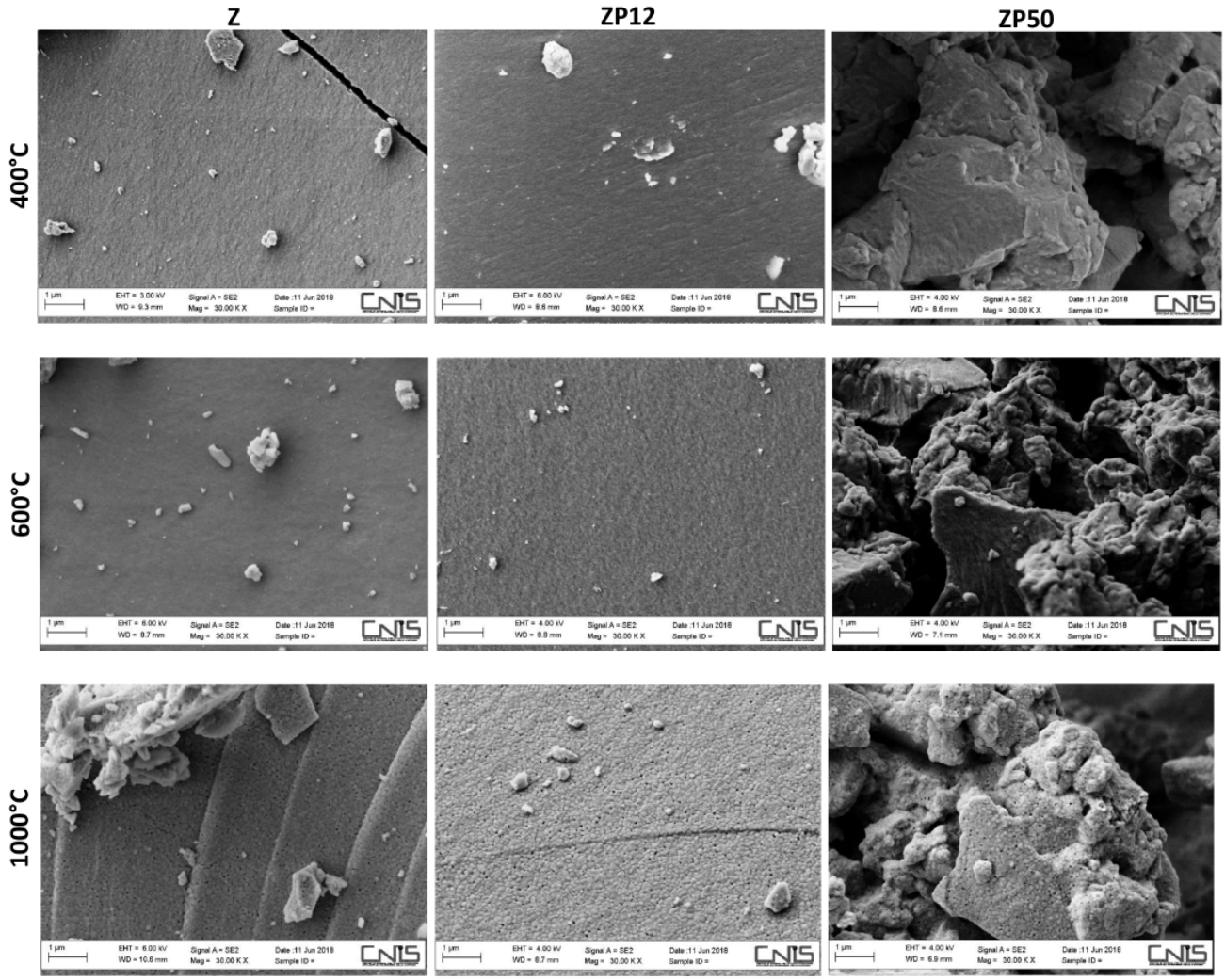

Figure 6)

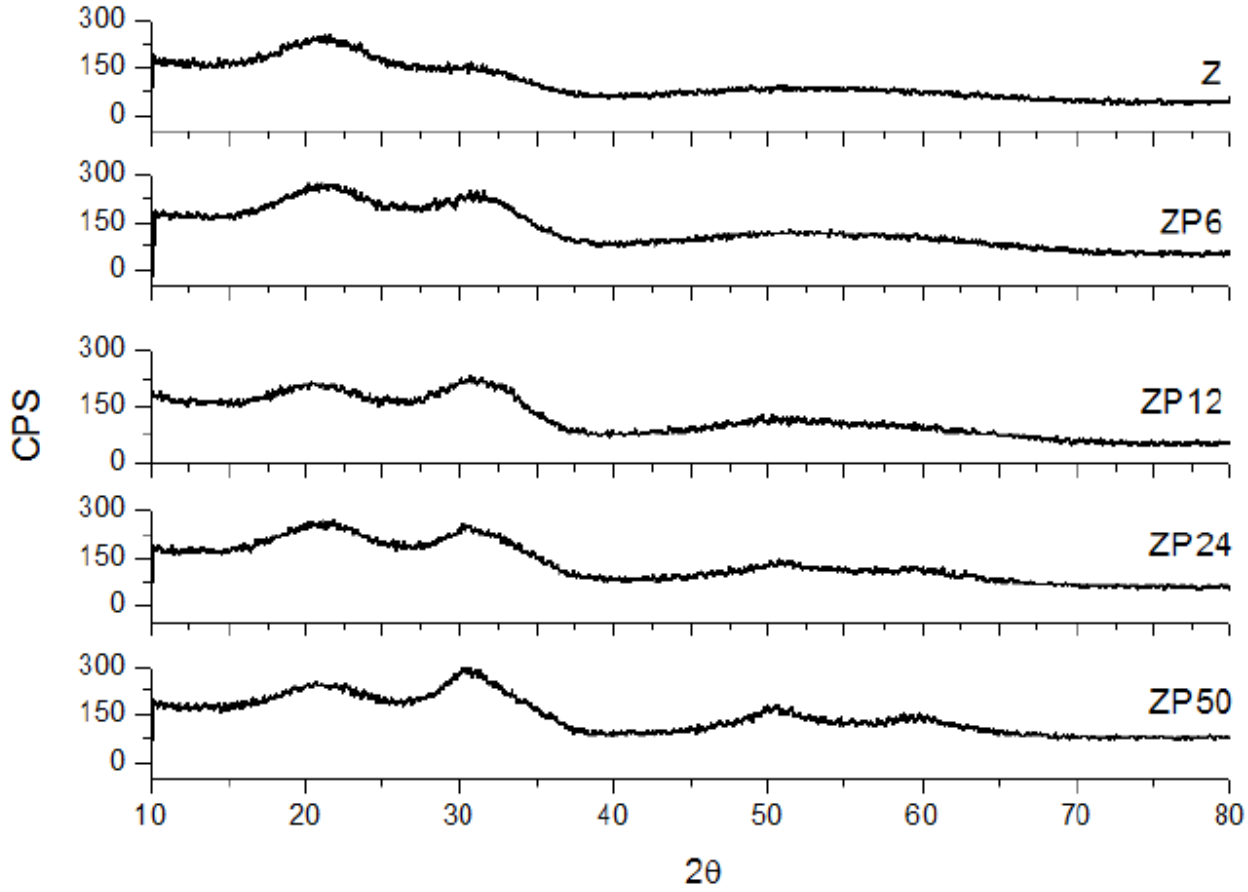

Figure 7)

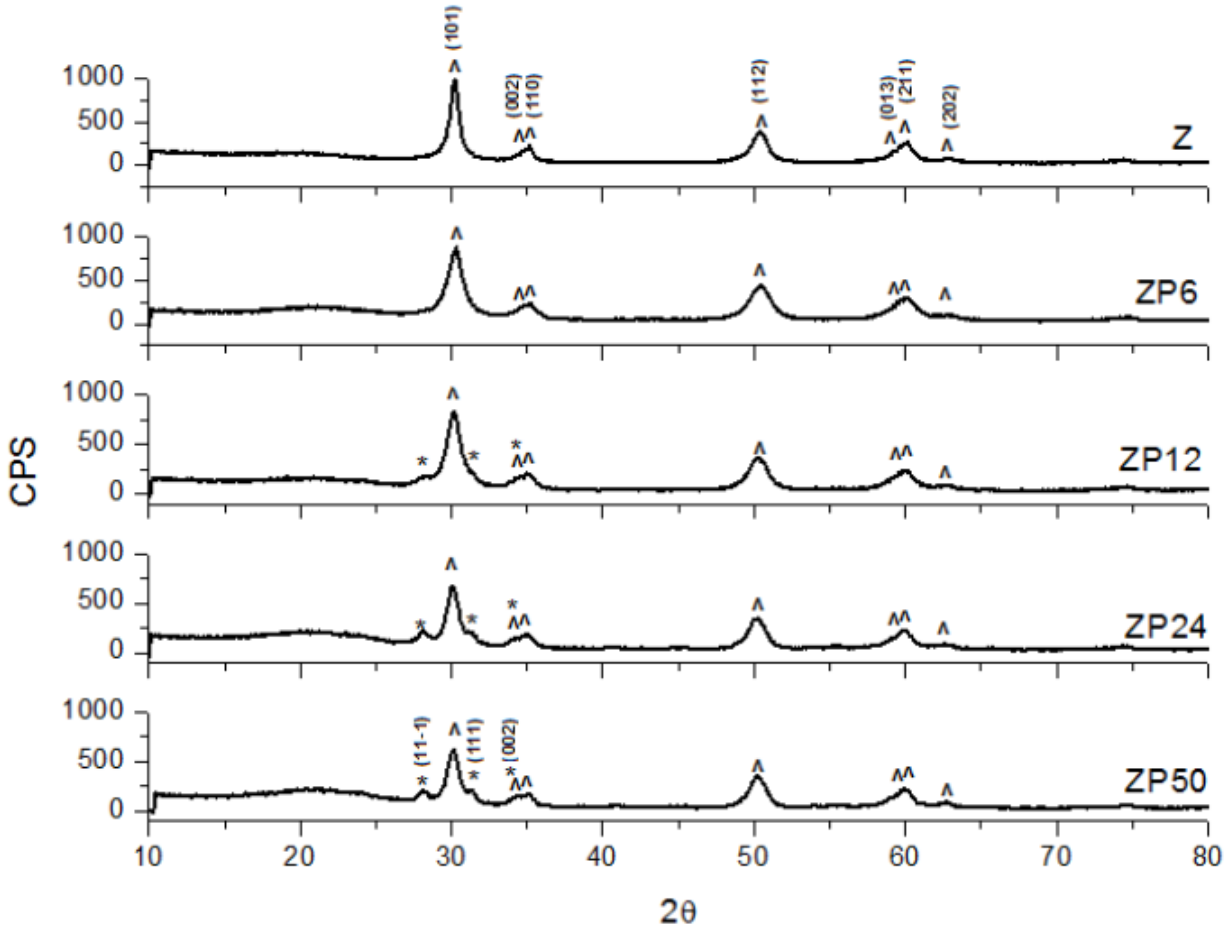
(101)
(002)
(110)
(112)
(013)
(211)
(202)
Z
ZP6
ZP12
ZP24
ZP50
(11-1)
(111)
(002)
1000
500
0
CPS
10
20
30
40
50
60
70
80
2θ

Figure 8)

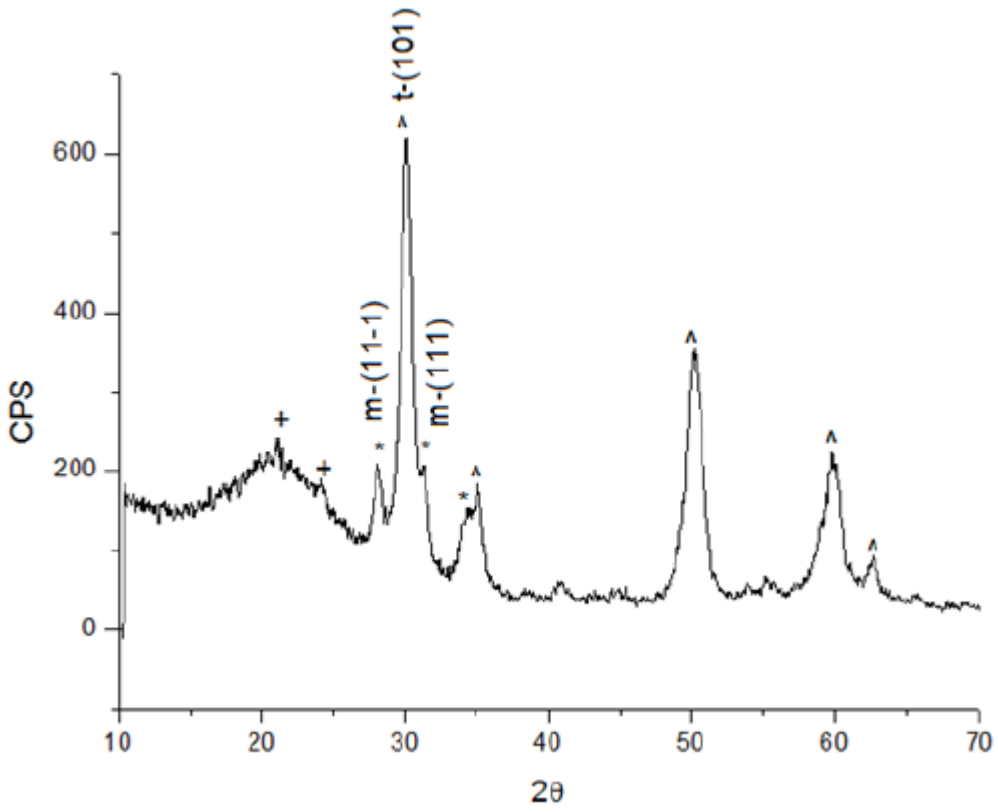

Figure 9)

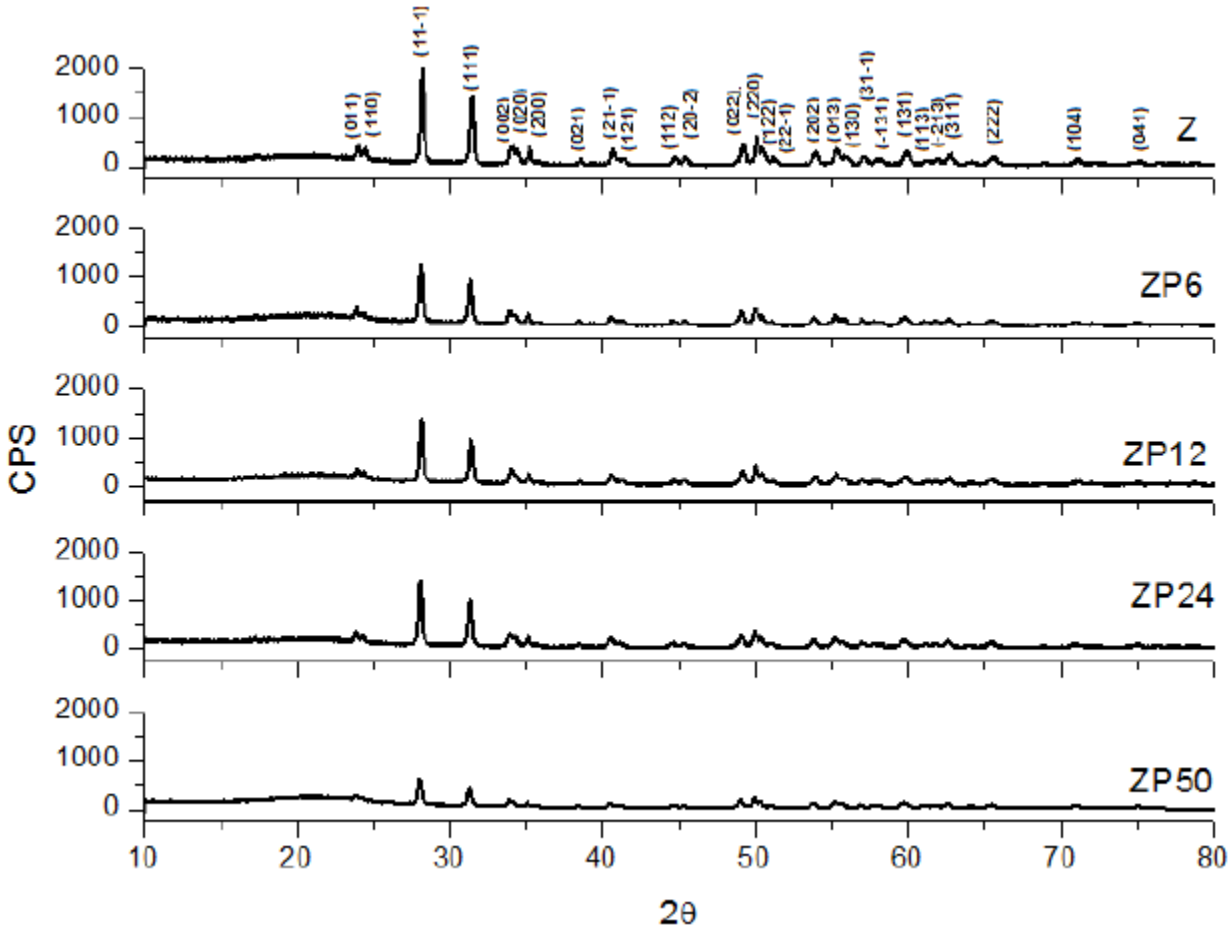
(011)
(110)
(11-1)
(111)
(002)
(020)
(200)
(021)
(21-1)
(121)
(112)
(20-2)
(022)
(220)
(122)
(22-1)
(202)
(013)
(130)
(31-1)
(-131)
(131)
(113)
(-213)
(311)
(222)
(104)
(041)
Z
ZP6
ZP12
ZP24
ZP50
2000
1000
0
CPS
10
20
30
40
50
60
70
80
2θ

Figure 10)

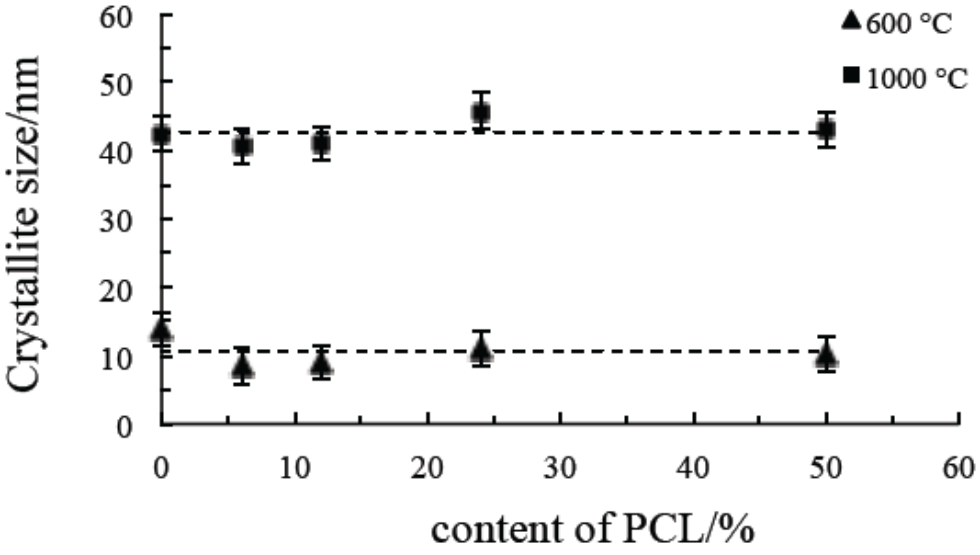
600 °C
1000 °C
Crystallite size/nm
content of PCL/%
0
10
20
30
40
50
60